



HAL
open science

Clustering Six Electrons within “Dawson-Like” Polyoxometalate: An Open Route toward Its Post-functionalization

Gabrielle Mpacko Priso, Mohamed Haouas, Nathalie Leclerc, Clément Falaise,
Emmanuel Cadot

► **To cite this version:**

Gabrielle Mpacko Priso, Mohamed Haouas, Nathalie Leclerc, Clément Falaise, Emmanuel Cadot. Clustering Six Electrons within “Dawson-Like” Polyoxometalate: An Open Route toward Its Post-functionalization. *Angewandte Chemie International Edition*, 2023, 62 (49), 10.1002/anie.202312457. hal-04334508

HAL Id: hal-04334508

<https://hal.science/hal-04334508>

Submitted on 22 Dec 2023

HAL is a multi-disciplinary open access archive for the deposit and dissemination of scientific research documents, whether they are published or not. The documents may come from teaching and research institutions in France or abroad, or from public or private research centers.

L'archive ouverte pluridisciplinaire **HAL**, est destinée au dépôt et à la diffusion de documents scientifiques de niveau recherche, publiés ou non, émanant des établissements d'enseignement et de recherche français ou étrangers, des laboratoires publics ou privés.



Distributed under a Creative Commons Attribution - NonCommercial - NoDerivatives 4.0
International License

VIP **Polyoxometalates** Very Important Paper

 How to cite: *Angew. Chem. Int. Ed.* **2023**, *62*, e202312457
 doi.org/10.1002/anie.202312457

Clustering Six Electrons within “Dawson-Like” Polyoxometalate: An Open Route toward Its Post-functionalization

Gabrielle Mpacko Priso, Mohamed Haouas, Nathalie Leclerc, Clément Falaise,* and Emmanuel Cadot

Dedicated to Michael T. Pope on the occasion of its 90th anniversary

Abstract: Super-reduction of polyoxometalates (POMs) in solution is of fundamental interest for designing innovative energy storage systems. In this article, we show that the “Dawson-like” POM can undergo a disproportionation process during its massive electron uptake, leading to species containing three metal-metal bonds as evidenced by X-ray diffraction, multi-nuclear magnetic resonance spectroscopy (¹H and ¹⁸³W NMR), extended X-ray absorption fine structure (EXAFS), UV/Vis, and voltammetry techniques. This result indicates that electron storing within metal-metal bonds is not a unique property of Keggin-type POM as postulated since the 70s. Besides, we demonstrate that the presence of an electron-rich triad in the “Dawson-like” POM allows its post-functionalization with additional tungstate ions, generating a chiral molecule that is also the largest W^{IV}-containing POMs known to date.

Polyoxometalates (POMs) represent an extensive class of anionic molecular oxides of early transition metals (mostly V, Mo, W)^[1] that have been recently identified as appealing redox mediators for applications in decoupled water-splitting systems, electro-organic synthesis, and redox-flow batteries (RFBs).^[2–6] In the latter domain, their use has made it possible to achieve energy densities surpassing those of industry-leading RFBs.^[7–9] Although POMs are strongly reduced during the charging of RFBs, the electron-storage mechanism within POMs remains poorly understood.^[10,11] Filling this lack of knowledge is crucial to lay the foundations of rational design of POMs-based RFBs, and more generally energy storage/conversion systems in which POMs are used either as electron reservoirs or electron

shuttles. In context, the first primary question concerns the structural elucidation of super-reduced species, and the second one consists of discovering the potential structure-reducibility relationships.

Super-reduction of POMs in water is systematically coupled with protonation processes provoking intricate phenomena.^[7,12,13] For instance, the massive electron uptake within the Dawson-type POM [P₂W₁₈O₆₂]^{6–} is associated with protonation processes that cause the formation of metastable aggregates, which surprisingly produce H₂ when they are diluted in solution.^[10] Another curious fact is that multiple proton-coupled reductions of Keggin-type anions [XW₁₂O₄₀]^{n–} (X = Si, B, or H₂) offer the possibility to store up to two electrons per metal center. Actually, this class of super-reduced POMs commonly referred to as “*browns*” or “*heteropoly browns*” owing to their brownish color, exhibit one of their four edge-sharing trimetallic units which store both six electrons and six protons.^[14–16] Within this electron-rich unit, the metal centers M^{IV} are connected through metal-metal bonds. Although the first descriptions of this clustering process were reported in the 70s,^[17,18] no other POM architecture has been identified to store electrons through a similar mechanism.^[11,19] This statement is rather surprising, since hundreds of POMs are built from metal-oxo fragments derived from a Keggin-type structure, and could therefore be subjected to a comparable reduction pathway.

Examining the super-reduction process of [H₂AsW₁₈O₆₀]^{7–} (noted H₂AsW₁₈-0; see Figure 1), a representative member of “Dawson-like” POMs [X₂W₁₈O₆₀]^{n–} (X = H₂, As, Sb, Bi, S, Se) that are built from two joined trivacant Keggin-type motifs {XW₉O₃₃}, we observed this POM is also capable of storing electrons in metal-metal bounded triad. In this communication, we report this finding that opens the way to a reconceptualization of the massive electron storage in POMs. Furthermore, we point out that the six-electron reduced POM [H₂AsW^{VI}₁₅W^{IV}₃O₅₇(H₂O)₃]^{7–} can be post-functionalized with additional tungsten centers, resulting in a chiral species [H₄AsW^{VI}₂₃W^{IV}₃O₈₅(H₂O)]^{13–} that is the largest W^{IV}-containing POM known to date (see Figure 1).

We have prepared a water-soluble salt of the eclipsed isomer of H₂AsW₁₈-0 (C_{3v} symmetry). In brief, the synthesis is similar to those reported for the straggled form,^[20] except that we prolonged the heating to favor the thermodynamic stable form (see Supporting Information for details).

[*] G. M. Priso, Dr. M. Haouas, Dr. N. Leclerc, Dr. C. Falaise, Prof. Dr. E. Cadot
 Institut Lavoisier de Versailles, CNRS, UVSQ, Université Paris-Saclay
 45 avenue des Etats-Unis, 78035, Versailles (France)
 E-mail: clement.falaise@uvsq.fr

© 2023 The Authors. Angewandte Chemie International Edition published by Wiley-VCH GmbH. This is an open access article under the terms of the Creative Commons Attribution Non-Commercial NoDerivs License, which permits use and distribution in any medium, provided the original work is properly cited, the use is non-commercial and no modifications or adaptations are made.

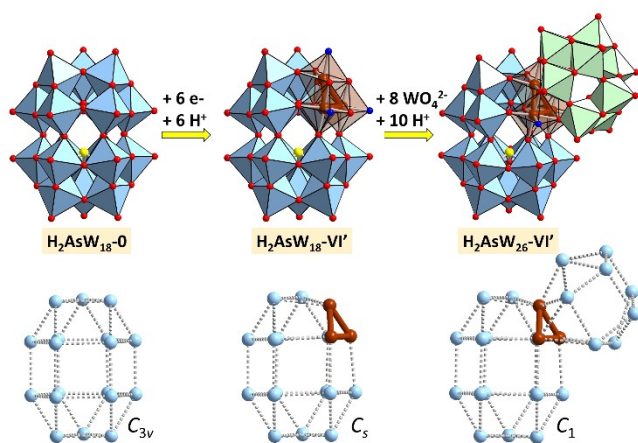


Figure 1. Electrosynthesis of super-reduced “Dawson-like” POM $[\text{H}_2\text{AsW}_{15}\text{W}^{\text{VI}}_3\text{O}_{57}(\text{H}_2\text{O})_3]^{7-}$ ($\text{H}_2\text{AsW}_{18}\text{-VI}'$; isolated as a mixed Na/Rb salt) and its inorganic post-functionalization to prepare $[\text{H}_4\text{AsW}_{23}\text{W}^{\text{VI}}_3\text{O}_{85}(\text{H}_2\text{O})]^{13-}$ ($\text{H}_2\text{AsW}_{26}\text{-VI}'$; isolated as a mixed K/Rb salt). Polyhedral representation (first row) and topological representation (second row) showing the contraction and symmetry breaking induced by both the clustering process and the functionalization. Color code: light-blue polyhedra, W^{VI} of “Dawson-like” fragment; brown polyhedra, W^{VI} , green polyhedra, W^{VI} of the octameric fragment; red spheres, O; blue spheres, terminal water molecules; yellow spheres, As^{III} .

$\text{H}_2\text{AsW}_{18}\text{-0}$ has been characterized by single-crystal X-ray diffraction, multinuclear NMR (^1H and ^{183}W), infrared spectroscopy, and elemental analysis (see Figure S1–S4 and Table S1 in the ESI). To the best of our knowledge, all previous electrochemical studies of Dawson-like POM were only performed in organic solvents.^[21] The redox behavior of $\text{H}_2\text{AsW}_{18}\text{-0}$ in aqueous solution has been investigated. At pH 5, the cyclic voltammogram consists of four well-separated reversible waves (see Figure 2 and S5). The two first events (labeled A and B) are monoelectronic processes while the two others (C and D) involve two electrons. Increasing the acidity of the media provokes continuous

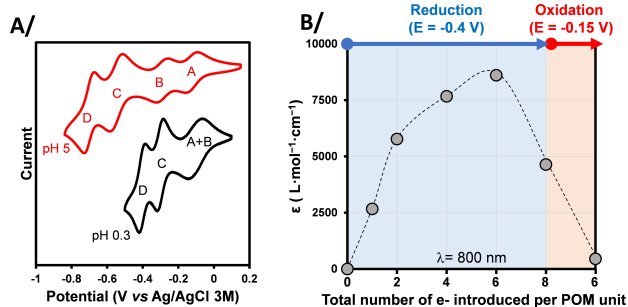


Figure 2. A/ Cyclic voltammograms of $\text{H}_2\text{AsW}_{18}\text{-0}$ in aqueous solution at pH 0.3 (black curve) and pH 5 (red curve). [POM] = 1 mM; WE: glassy carbon; REF: Ag/AgCl; CE: Pt; scan rate: 100 mV/s. B/ Evolution of molar attenuation coefficient ϵ at $\lambda = 800$ nm during the bulk electrolysis processes at controlled potential (pH 0.3), allowing the introduction of eight electrons per POM unit when $E = -0.4$ V, and then the formation of the $\text{H}_2\text{AsW}_{18}\text{-VI}'$ when $E = -0.15$ V.

moving of C and D in a positive direction by about -60 and -100 mV/pH unit (Figure S6), respectively. Below pH 3, event B moves by -60 mV/pH and tends to merge with the first wave at pH 0.3. This electrochemical behavior highlights that the electron transfer in $\text{H}_2\text{AsW}_{18}\text{-0}$ is proton-coupled.

To determine how electrons are stored in $\text{H}_2\text{AsW}_{18}\text{-0}$, we attempted to prepare the four-electron reduced species in dilute H_2SO_4 using bulk electrolysis at controlled potential ($E = -0.4$ V vs Ag/AgCl). Surprisingly, according to coulometry measurement, this treatment produces a dark blue solution corresponding to eight electron-reduced POMs. This suggests the existence of a disproportionation process of the four-electron reduced POM. The reduction process has been monitored by UV/Vis measurements. The results show that the intensity of the broad band located at 800 nm corresponding to intervalence charge transfers ($\text{W}^{\text{V}} \rightarrow \text{W}^{\text{VI}}$), increases with the addition of six equivalents of electrons per POM (Figure 2B and S7). It is important to note that a dramatic decrease in the intensity is observed when eight electrons are introduced into the POM unit. This reflects a part of additional electrons becomes localized within the tungsten-oxo framework. The controlled oxidation ($E = -0.15$ V) of the solution containing POM reduced by eight electrons led to a greenish solution that contains a six-electron reduced POM notated $\text{H}_2\text{AsW}_{18}\text{-VI}'$ with low ϵ at 800 nm. Then, this reduced POM has been isolated using RbCl and recrystallized in NaCl solution (see Supporting Information for details), giving crystals of $\text{Rb}_{5.75}\text{Na}_{1.25}[\text{H}_2\text{AsW}_{15}\text{W}^{\text{VI}}_3\text{O}_{57}(\text{H}_2\text{O})_3] \cdot 18\text{H}_2\text{O}$ ($\text{Rb}_{5.75}\text{Na}_{1.25} \cdot \text{H}_2\text{AsW}_{18}\text{-VI}' \cdot 18\text{H}_2\text{O}$). We noticed that the combination of cations (Na^+ and Rb^+) is necessary to crystallize single-crystal suitable for X-ray diffraction analysis. The chemical formula of the compound was confirmed by TGA, redox titration (Figure S8), and elemental analysis.

The single-crystal diffraction analysis of $\text{Rb}_{5.75}\text{Na}_{1.25} \cdot \text{H}_2\text{AsW}_{18}\text{-VI}' \cdot 18\text{H}_2\text{O}$ revealed the polyanion $[\text{H}_2\text{AsW}_{15}\text{W}^{\text{VI}}_3\text{O}_{57}(\text{H}_2\text{O})_3]^{7-}$ crystallizes in centrosymmetric space group $P-1$ (Table S2). It consists of a metal-metal bonded triad $\{\text{W}^{\text{IV}}_3\text{O}_{13}\}$ located on the $\{\text{H}_2\text{W}_9\}$ side while the $\{\text{AsW}_9\}$ moiety remained almost unchanged (Figure 3A). This produces a contracted dawsonoid topology (Figure 1) which is quite analogous to that observed in the hybrid compound $[\text{H}_2\text{Sb}_3\text{Mo}^{\text{IV}}_3\text{Mo}^{\text{VI}}_{15}\text{O}_{57}(\text{pyridine})_3]^-$ prepared from partial oxidation of trinuclear Mo^{IV} -based cluster during a solvothermal treatment.^[11,22] Within $\{\text{W}^{\text{IV}}_3\text{O}_{13}\}$, the homometallic metal-metal bond length is in the range 2.53–2.55 Å as commonly observed in trinuclear clusters.^[23,24] The distance between the W^{IV} center and the terminal oxygen atoms is in the range of 2.16–2.2 Å, indicating that each W^{IV} is coordinated with a water molecule. Although the two protons trapped within the $\{\text{H}_2\text{W}_9\}$ subunit are delocalized on the three μ_3 -oxygen atoms of the non-reduced triads $\{\text{W}^{\text{VI}}_3\text{O}_{13}\}$ when the POM is not reduced, BVS calculations suggest the two internal H^+ of $\text{H}_2\text{AsW}_{18}\text{-VI}'$ become mostly localized on the μ_3 -oxygen atoms of the non-reduced triad (Table S3). The differences in structural characteristics between $\text{H}_2\text{AsW}_{18}\text{-VI}'$ and $\text{H}_2\text{AsW}_{18}\text{-0}$ are also seen in the IR spectra of the solid products, especially in the region

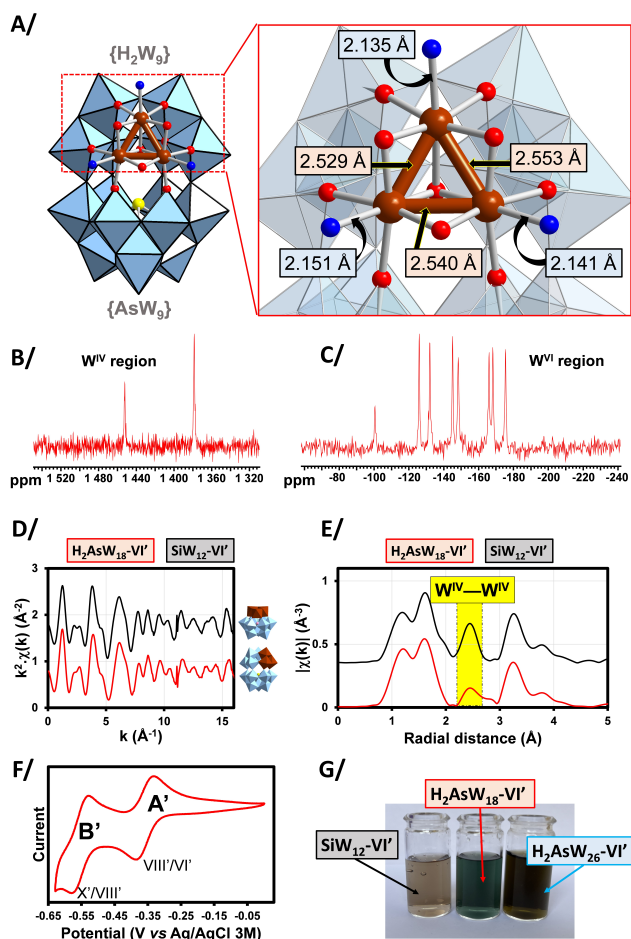


Figure 3. A/ Illustration of the X-ray structure of $\text{H}_2\text{AsW}_{18}\text{-VI}'$ with a focus on the metal-metal bonded triad. B and C/ ^{183}W NMR spectrum of the $\text{H}_2\text{AsW}_{18}\text{-VI}'$ in aqueous solution. D/ Comparison of the EXAFS spectra of $\text{H}_2\text{AsW}_{18}\text{-VI}'$ and $[\text{SiW}_{12}^{\text{VI}}\text{O}_{37}(\text{H}_2\text{O})_3]^{4-}$ (notated $\text{SiW}_{12}\text{-VI}'$) in aqueous solution. E/ Comparison of the Fourier transforms of $\text{H}_2\text{AsW}_{18}\text{-VI}'$ and $\text{SiW}_{12}\text{-VI}'$. F/ Cyclic voltammogram of $\text{H}_2\text{AsW}_{18}\text{-VI}'$ in aqueous solution in dilute H_2SO_4 (0.5 M), $[\text{POM}] = 2$ mM; WE: glassy carbon; REF: Ag/AgCl; CE: Pt; scan rate: 100 mV/s. G/ Photograph of the aqueous solutions of $\text{SiW}_{12}\text{-VI}'$, $\text{H}_2\text{AsW}_{18}\text{-VI}'$ and $\text{H}_2\text{AsW}_{26}\text{-VI}'$, highlighting the color of the POM containing $\{\text{W}^{\text{IV}}_3\text{O}_{13}\}$ are strongly affected by their local environment.

corresponding to the stretching modes of W–O–W junctions (Figure S9).

The clustering process induces a decrease in symmetry from C_{3v} for $\text{H}_2\text{AsW}_{18}\text{-0}$ to C_s for $\text{H}_2\text{AsW}_{18}\text{-VI}'$, as confirmed by the ^{183}W NMR study. Indeed, four resonances (relative intensity = 1:1:2:2; see Figure S3) are observed for the oxidized form, while the spectrum of $\text{H}_2\text{AsW}_{18}\text{-VI}'$ exhibits ten resonances. The eight resonances of W^{VI} centers (relative intensity = 1:2:2:2:2:2:2:2) are observed in the range -100 to -175 ppm (Figure 3C), whereas the two signals of reduced W^{IV} centers (relative intensity = 1:2) are strongly deshielded and are more precisely observed at $+1452$ and $+1378$ ppm (Figure 3B), in typical chemical shift range for W^{IV} . We note that the nature of the counteranions (H^+ or Rb^+) affects slightly the ^{183}W signals (Fig-

ure S10). The ^1H NMR spectrum of $\text{H}_2\text{AsW}_{18}\text{-VI}'$ shows a singlet at 6.6 ppm (Figure S11) that is related to the two internal equivalent protons of the reduced subunit $\{\text{H}_2\text{W}^{\text{IV}}_3\text{W}^{\text{VI}}_6\}$ (a singlet is observed at 5.2 ppm for the $\text{H}_2\text{AsW}_{18}\text{-0}$, see Figure S3).

The compound $\text{H}_2\text{AsW}_{18}\text{-VI}'$ was then characterized in solution using EXAFS analysis and compared with that measured for the classical “heteropoly brown” $[\text{SiW}_{12}^{\text{VI}}\text{O}_{37}(\text{H}_2\text{O})_3]^{4-}$ also containing a metal-metal bonded triad (Figure 3D, 3E, and S12). The two compounds show similar Fourier transforms (uncorrected for phase shift) with five main contributions. The first two are located between 1 and 2 Å and correspond to the first oxygen coordination shell. The third one, pointed at ~ 2.5 Å, is the signature of three $\text{W}^{\text{IV}}\text{-W}^{\text{IV}}$ bonds contained in the super-reduced triad. In contrast, the peak of the distance between W^{VI} centers belonging to $\{\text{W}^{\text{VI}}_3\text{O}_{13}\}$ is observed at ~ 3.3 Å. The last peak is observed at ~ 3.8 Å and corresponds to the shortest distances between two tungsten centers from distinct trimetallic units. The only dissimilarity between EXAFS data of the two super-reduced POMs is the relative intensity of the peaks at ~ 2.5 and ~ 3.3 Å. This is simply due to the difference of $\{\text{W}^{\text{VI}}_3\text{O}_{13}\}/\{\text{W}^{\text{IV}}_3\text{O}_{13}\}$ ratio in the two compounds.

At pH 0.3, the cyclic voltammogram of $\text{H}_2\text{AsW}_{18}\text{-VI}'$ exhibits two pseudo-reversible di-electronic redox waves (labeled A' and B', see Figure 3F). These two redox events vary with pH, meaning these two events involved concomitantly protonation processes (Figure S13). It is worth noting that the A' event is observed at the same potential as the C event of the non-reduced POM. The oxidation of $\text{H}_2\text{AsW}_{18}\text{-VI}'$ into $\text{H}_2\text{AsW}_{18}\text{-0}$ is characterized by a non-reversible anodic large peak spreading from 0.3 to 1 V and the swiping back-cycling revealed that the non-reduced POMs is fully restored, as evidenced by the reappearance of the events A and B (Figure S14).

In the light of all these results, we conclude that the “Dawson-like” POM $[\text{H}_2\text{AsW}_{18}\text{O}_{60}]^{7-}$ retains its original structure during super-reduction without molecular transformation, but accepting the confinement of six electrons in one trimetallic unit of the $\{\text{H}_2\text{W}_9\}$ subunit. The resulting entity $\text{H}_2\text{AsW}_{18}\text{-VI}'$ represents the first example of POM containing $\{\text{W}^{\text{IV}}_3\text{O}_{13}\}$ motif outside the classical “heteropoly browns”, however it differs notably due to its green color in solution (Figure 3G), suggesting that the electronic transitions of $\{\text{W}^{\text{IV}}_3\text{O}_{13}\}$ are slightly altered by their local environment. More importantly, our results allow us to demonstrate that the clustering process occurs through the disproportionation of the four-electron reduced form in acid solution ($2 \text{IV} \rightarrow \text{II} + \text{VI}'$). The instability of the four-electron reduced form leads to the two-electron reduced POM and $\text{H}_2\text{AsW}_{18}\text{-VI}'$. Nevertheless, since the first $E_{1/2}$ of $\text{H}_2\text{AsW}_{18}\text{-VI}'$ is almost identical to the potential needed to generate the four-electron reduced derivative, the bulk electrolysis of $\text{H}_2\text{AsW}_{18}\text{-0}$ at -0.4 V further continues up to eight electrons per POM, as evidenced experimentally. Therefore, partial oxidation is required to isolate the six-electron reduced POM $\text{H}_2\text{AsW}_{18}\text{-VI}'$.

The presence of an electron-rich triad in the “Dawson-like” POM may offer a means of post-functionalizing for the first time this class of POMs whose their lacunary entities, the usual precursors for the design of new POM-based architectures,^[25–28] remain elusive. Inspired by the pioneering work of Pope et al.,^[29] we have successfully used $\text{H}_2\text{AsW}_{18}\text{-VI}'$ as an inorganic precursor to form the largest POM containing W^{IV} centers reported to date. The resulting POM is prepared from an aqueous solution containing $\text{H}_2\text{AsW}_{18}\text{-VI}'$ and tungstate ions at pH 4 (see Supporting Information for details). The precipitation with KCl and the recrystallization in a minimum of water lead to the compound $\text{K}_{10}\text{RbH}_2[\text{H}_4\text{AsW}_{23}^{\text{VI}}\text{W}_{3}^{\text{IV}}\text{O}_{85}(\text{H}_2\text{O})]\cdot 9\text{H}_2\text{O}$ (notated $\text{K}_{10}\text{RbH}_2\cdot\text{H}_2\text{AsW}_{26}\text{-VI}'\cdot 9\text{H}_2\text{O}$). Single crystal X-ray diffraction analysis reveals that the polyanion $[\text{H}_4\text{AsW}_{23}^{\text{VI}}\text{W}_{3}^{\text{IV}}\text{O}_{85}(\text{H}_2\text{O})]^{13-}$ (C_1 symmetry) can be viewed as a six-electron reduced “Dawson-like” POM linked to a β -Keggin $\{\text{W}_8\}$ defect fragment (Figure 4A). This $\{\text{W}_8\}$ unit is a well-known structural motif composed of two trimers bonded by a dimeric unit.^[29,30,30] The $\{\text{W}^{\text{IV}}_3\text{O}_{13}\}$ triad is linked to two trimer units of the octameric unit through four oxygen atoms. Two of them, that were a terminal aqua group in $\text{H}_2\text{AsW}_{18}\text{-VI}'$, bridge one reduced W^{IV} center ($d_{\text{W-O}} = 2.03 \text{ \AA}$) to one W^{VI} center ($d_{\text{W-O}} = 1.82\text{--}1.85 \text{ \AA}$) belonging to $\{\text{W}_8\}$ (Figure 4A). The two other oxygen atoms are μ_3 -oxo groups connecting two W^{IV} centers ($d_{\text{W-O}} = 1.98\text{--}2.04 \text{ \AA}$) with one W^{VI} center ($d_{\text{W-O}} = 2.08\text{--}2.16 \text{ \AA}$). The remaining oxygen atoms of $\{\text{W}^{\text{IV}}_3\text{O}_{13}\}$ exhibit W–O bond lengths comparable to those of the parent anion $\text{H}_2\text{AsW}_{18}\text{-VI}'$. We also note that

the homometallic metal-metal bond lengths ($d_{\text{W-W}} = 2.57\text{--}2.60 \text{ \AA}$) are slightly larger in $\text{H}_2\text{AsW}_{26}\text{-VI}'$. Although $\text{H}_2\text{AsW}_{26}\text{-VI}'$ displays strong structural analogies with compounds containing the $\{\text{H}_2\text{W}_8\}$ unit grafted on six-electron reduced Keggin anions,^[29] particularly with regard to interatomic distances, the structural properties differ considerably. Indeed, $\text{H}_2\text{AsW}_{26}\text{-VI}'$ represents a rare example of an all-inorganic chiral POM.^[31,32] The grafting of the octameric unit on the reduced triad $\{\text{W}^{\text{IV}}_3\text{O}_{13}\}$ induces a modification of the electronic properties as evidenced by the color change from green for $\text{H}_2\text{AsW}_{28}\text{-VI}'$ to brown for $\text{H}_2\text{AsW}_{26}\text{-VI}'$ (Figure 3F).

To go further, we studied the structure of $\text{H}_2\text{AsW}_{26}\text{-VI}'$ in solution by ^1H and ^{183}W NMR (Figure 4, Figure S15 and S16). In short, the ^{183}W NMR spectrum recorded in the low-frequency region displays 22 resolved resonances over relatively a large chemical shift range (from +2 to -201 ppm). Of the 22 peaks, 21 resonances have the same intensity, while one resonance at $\delta -163.5$ ppm shows a doubled intensity, consistent with an accidental degeneracy of two signals of equal intensity (Figure 4B). Therefore, this part of the ^{183}W NMR spectrum is interpreted as a 23-line spectrum, as expected for the pure solution of $\text{H}_2\text{AsW}_{26}\text{-VI}'$. The two W signals located at about 0 ppm should correspond to the W centers of the outer W_2O_{10} group of the β -Keggin fragment. In the region corresponding to the reduced W centers (Figure 4C), we note the presence of three signals observed at +1544, +1620, and +1831 ppm, due to the three non-equivalent W^{IV} sites in the reduced triad. Furthermore, the ^1H NMR spectrum of $\text{H}_2\text{AsW}_{26}\text{-VI}'$ shows two signals with relative intensity 1:1 corresponding to the two H^+ trapped inside the chiral “Dawson-like” capsule (Figure 4D), as a consequence of the symmetry lowering to the C_1 point group.

In summary, super-reduction of “Dawson-like” POM $\text{H}_2\text{AsW}_{18}\text{-0}$ in acidic solution leads to a disproportionation process of the four electron-reduced entities, resulting in the formation of POM containing a metal-metal bounded triad. This result represents a paradigm shift, demonstrating for the first time that electron storage in metal-metal bonds is not limited to the Keggin-type POMs, but could be extended to all POMs containing the $\{\text{W}^{\text{VI}}_3\text{O}_{13}\}$ triad. This paves the way for a reexamination of the super-reduction of POMs built from the $\{\text{M}^{\text{VI}}_3\text{O}_{13}\}$ triads with $\text{M} = \text{Mo}$ or W under the prism of the clustering process.

Furthermore, we also demonstrated that the post-functionalization of super-reduced “Dawson-like” POM leads to a chiral molecule with one W^{IV} center linked to a water molecule that is expected labile enough to create coordinatively unsaturated sites. This could open up new prospects for asymmetric catalysis.

Supporting Information

The authors have cited additional references within the Supporting Information.^[33,34]

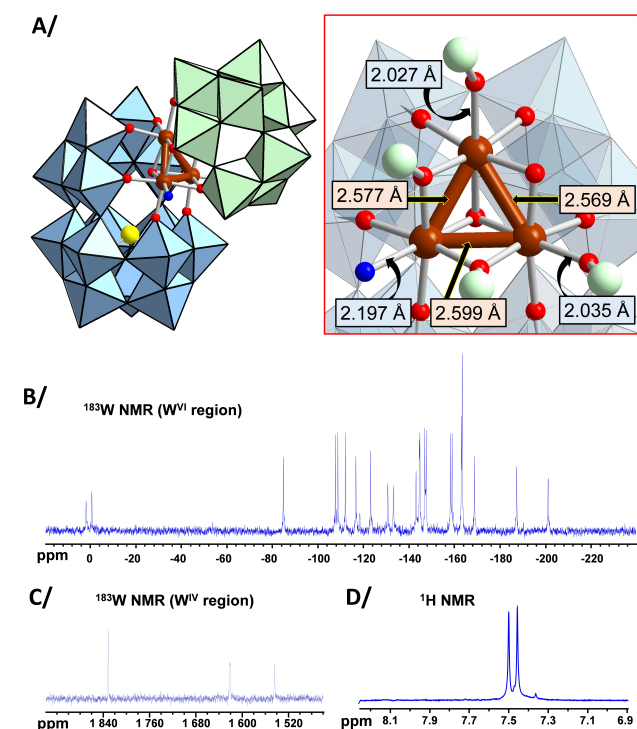


Figure 4. A/Illustration of the X-ray structure of $\text{H}_2\text{AsW}_{26}\text{-VI}'$ with a focus on the metal-metal bonded triad. B, C and D/Multinuclear NMR spectra (^1H and ^{183}W) of the $\text{H}_2\text{AsW}_{26}\text{-VI}'$ in aqueous solution.

Acknowledgements

GMP acknowledges the University of Paris-Saclay for her Ph.D. grant funding. We acknowledge SOLEIL Synchrotron for providing beamtime and synchrotron radiation facilities on the ROCK beamline for the EXAFS studies. We especially thank Dr. V. Briois for assistance in using the ROCK beamline and for fruitful discussions. The authors gratefully acknowledge the financial support from the CNRS (EMERGENCE@INC2023), the UVSQ, the Paris Ile-de-France Region-DIM “Respire”, the French National Research Agency as part of the “Investissements d’Avenir” program (Labex Charm3at, ANR-11-LABX-0039-grant).

Conflict of Interest

The authors declare no conflict of interest.

Data Availability Statement

The data that support the findings of this study are available from the corresponding author upon reasonable request.

Keywords: Metal-Metal Bonds · Polyoxometalates · Post-Functionalization · Structural Elucidation · Super-Reduction

- [1] M. Pope, *Heteropoly and Isopoly Oxometalates*, Springer-Verlag, Berlin, Heidelberg, **1983**.
- [2] B. Rausch, M. D. Symes, G. Chisholm, L. Cronin, *Science* **2014**, *345*, 1326–1330.
- [3] J. M. Cameron, C. Holc, A. J. Kibler, C. L. Peake, D. A. Walsh, G. N. Newton, L. R. Johnson, *Chem. Soc. Rev.* **2021**, *50*, 5863–5883.
- [4] A. D. Stergiou, M. D. Symes, *Catal. Today* **2022**, *384–386*, 146–155.
- [5] S. Amthor, S. Knoll, M. Heiland, L. Zedler, C. Li, D. Nauroozi, W. Tobiaschus, A. K. Mengele, M. Anjass, U. S. Schubert, B. Dietzek-Ivanšić, S. Rau, C. Streb, *Nat. Chem.* **2022**, *14*, 321–327.
- [6] L. E. VanGelder, A. M. Kosswattaarachchi, P. L. Forrestel, T. R. Cook, E. M. Matson, *Chem. Sci.* **2018**, *9*, 1692–1699.
- [7] J.-J. Chen, M. D. Symes, L. Cronin, *Nat. Chem.* **2018**, *10*, 1042–1047.
- [8] F. Ai, Z. Wang, N.-C. Lai, Q. Zou, Z. Liang, Y.-C. Lu, *Nat. Energy* **2022**, *7*, 417–426.
- [9] L. Yang, Y. Hao, J. Lin, K. Li, S. Luo, J. Lei, Y. Han, R. Yuan, G. Liu, B. Ren, J. Chen, *Adv. Mater.* **2022**, *34*, 2107425.
- [10] J.-J. Chen, L. Vilà-Nadal, A. Solé-Daura, G. Chisholm, T. Minato, C. Busche, T. Zhao, B. Kandasamy, A. Y. Ganin, R. M. Smith, I. Colliard, J. J. Carbó, J. M. Poblet, M. Nyman, L. Cronin, *J. Am. Chem. Soc.* **2022**, *144*, 8951–8960.
- [11] A. Kondinski, *Nanoscale* **2021**, *13*, 13574–13592.
- [12] T. Zhao, N. L. Bell, G. Chisholm, B. Kandasamy, D.-L. Long, L. Cronin, *Energy Environ. Sci.* **2023**, *16*, 2603–2610.
- [13] M. Sadakane, E. Steckhan, *Chem. Rev.* **1998**, *98*, 219–238.
- [14] K. Piepgrass, M. T. Pope, *J. Am. Chem. Soc.* **1987**, *109*, 1586–1587.
- [15] T. Yamase, E. Ishikawa, *J. Chem. Soc. Dalton Trans.* **1996**, 1619–1627.
- [16] C. Falaise, G. Mpacko Priso, N. Leclerc, M. Haouas, E. Cadot, *Inorg. Chem.* **2023**, *62*, 2494–2502.
- [17] G. Hervé, *Ann. Chim.* **1971**, 287–296.
- [18] J. P. Launay, *J. Inorg. Nucl. Chem.* **1976**, *38*, 807–816.
- [19] N. I. Gumerova, A. Rompel, *Nat. Chem. Rev.* **2018**, *2*, 0112.
- [20] Y. Jeannin, J. Martin-Frère, *Inorg. Chem.* **1979**, *18*, 3010–3014.
- [21] C. Busche, L. Vilà-Nadal, J. Yan, H. N. Miras, D.-L. Long, V. P. Georgiev, A. Asenov, R. H. Pedersen, N. Gadegaard, M. M. Mirza, D. J. Paul, J. M. Poblet, L. Cronin, *Nature* **2014**, *515*, 545–549.
- [22] F. Yu, L. Xu, *Dalton Trans.* **2019**, *48*, 17445–17450.
- [23] B. Modéc, P. Bukovec, *Inorg. Chim. Acta* **2015**, *424*, 226–234.
- [24] P. Chaudhuri, K. Wiegardt, W. Gebert, I. Jibril, G. Huttner, *Z. Anorg. Allg. Chem.* **1985**, *521*, 23–36.
- [25] T. J. R. Weakley, H. T. Evans, J. S. Showell, G. F. Tourné, C. M. Tourné, *J. Chem. Soc. Chem. Commun.* **1973**, 139–140.
- [26] C. Li, N. Mizuno, K. Yamaguchi, K. Suzuki, *J. Am. Chem. Soc.* **2019**, *141*, 7687–7692.
- [27] S. S. Amin, K. D. Jones, A. J. Kibler, H. A. Damian, J. M. Cameron, K. S. Butler, S. P. Argent, M. Winslow, D. Robinson, N. J. Mitchell, H. W. Lam, G. N. Newton, *Angew. Chem. Int. Ed.* **2023**, *62*, e202302446.
- [28] Q. Chang, X. Meng, W. Ruan, Y. Feng, R. Li, J. Zhu, Y. Ding, H. Lv, W. Wang, G. Chen, X. Fang, *Angew. Chem. Int. Ed.* **2022**, *61*, e202117637.
- [29] M. H. Dickman, T. Ozeki, J. Howard, T. Evans, C. Rong, G. B. Jameson, M. T. Pope, *J. Chem. Soc. Dalton Trans.* **2000**, 149–154.
- [30] B. S. Bassil, S. Nellutla, U. Kortz, A. C. Stowe, J. van Tol, N. S. Dalal, B. Keita, L. Nadjo, *Inorg. Chem.* **2005**, *44*, 2659–2665.
- [31] N. Leclerc-Laronze, J. Marrot, G. Hervé, R. Thouvenot, E. Cadot, *Chem. Eur. J.* **2007**, *13*, 7234–7245.
- [32] G. Lenoble, B. Hasenknopf, R. Thouvenot, *J. Am. Chem. Soc.* **2006**, *128*, 5735–5744.
- [33] O. V. Dolomanov, L. J. Bourhis, R. J. Gildea, J. a. K. Howard, H. Puschmann, *J. Appl. Crystallogr.* **2009**, *42*, 339–341.
- [34] G. M. Sheldrick, *Acta Crystallogr. Sect. A* **2015**, *71*, 3–8.

Manuscript received: August 24, 2023

Accepted manuscript online: October 13, 2023

Version of record online: November 6, 2023